JACS
JOURNAL OF THE AMERICAN CHEMICAL SOCIETY
Communication
pubs.acs.org/JACS

Inhibition of Charge Disproportionation of MnO_2 Electrocatalysts for Efficient Water Oxidation under Neutral Conditions

Toshihiro Takashima,[†,§] Kazuhito Hashimoto,*[,†,‡] and Ryuhei Nakamura*[,†]

[†]Department of Applied Chemistry, School of Engineering, The University of Tokyo, 7-3-1 Hongo, Bunkyo-ku, Tokyo 113-8656, Japan

[‡]ERATO/JST, HASHIMOTO Light Energy Conversion Project, Japan

Supporting Information

ABSTRACT: The development of Mn-oxide electrocatalysts for the oxidation of H_2O to O_2 has been the subject of intensive researches not only for their importance as components of artificial photosynthetic systems, but also as O_2-evolving centers in photosystem II. However, limited knowledge of the mechanisms underlying this oxidation reaction hampers the ability to rationally design effective catalysts. Herein, using *in situ* spectroelectrochemical techniques, we demonstrate that the stabilization of surface-associated intermediate Mn^{3+} species relative to charge disproportionation is an effective strategy to lower the overpotential for water oxidation by MnO_2. The formation of N−Mn bonds via the coordination of amine groups of poly(allylamine hydrochloride) to the surface Mn sites of MnO_2 electrodes effectively stabilized the Mn^{3+} species, resulting in an ∼500-mV negative shift of the onset potential for the O_2 evolution reaction at neutral pH.

Water oxidation is generally considered to be the bottleneck reaction in artificial photosynthetic systems[1−9] designed to produce hydrogen through proton reduction or convert carbon dioxide to liquid fuel because of the inherent difficulty of catalyzing the overall four-electron/four-proton reaction ($2H_2O \rightarrow 4H^+ + 4e^- + O_2$). However, the water oxidation reaction proceeds with extraordinary high catalytic activity in naturally occurring photosystem II (PSII), where a μ-oxo bridged tetrameric Mn cluster (Mn_4CaO_5) serves as the multielectron oxidation catalyst within a complex protein environment.[3,10−13] Thus, the Mn clusters of photosynthetic organisms have triggered extensive research efforts to develop efficient water oxidation catalysts composed of the inexpensive and abundant element Mn.[14−24] To date, there have been notable developments in relation to bioinspired water oxidation catalysts,[18−24] particularly Mn oxides, including simple and mixed-metal oxides, that have been demonstrated to function as effective electrocatalysts under strongly alkaline conditions. However, as the O_2-evolving activity of these Mn catalysts is markedly suppressed at neutral pH, a large electrochemical overpotential, ranging from 500 to 700 mV, is required for O_2 evolution.[2,24,25] For their successful application as components of artificial photosynthetic systems, it is essential to improve the water oxidation activity of Mn catalysts, particularly under neutral conditions. Nevertheless, few studies have investigated the mechanisms of water oxidation at the surface of Mn-oxide electrodes. Thus, it is unclear why the catalytic activity of Mn oxides sharply declines under neutral conditions and remains the subject of debate.[2,13]

Recently, we identified that an optical absorption band peak at 510 nm was generated for a Mn-oxide electrocatalyst during the catalytic cycle of water oxidation.[25] Measurement of *in situ* water oxidation current and optical absorption, and the results of a probe experiment using pyrophosphate (PP), have shown that the 510-nm absorption is assignable to d−d transition of surface-associated Mn^{3+} ions, which is formed by the electron injection from H_2O to anodically poised MnO_2 and acts as a precursor of the O_2 evolution reaction.[25] Notably, Mn^{3+} is unstable at pH <9 due to charge disproportionation (CD) that results in the formation of Mn^{2+} and Mn^{4+} ($2Mn^{3+} \rightarrow Mn^{2+} + Mn^{4+}$), but is effectively stabilized by comproportionation at high alkalinity.[13,26,27] Thus, the low water oxidation activity of Mn oxides under neutral conditions is attributable to the inherent instability of Mn^{3+}, whose accumulation at catalytic surfaces requires the electrochemical oxidation of Mn^{2+} at a potential of ∼1.4 V, as schematically illustrated in Figure 1.[25] On the basis of this proposed model, we hypothesize that the stabilization of Mn^{3+} relative to CD is essential for the development of Mn catalysts that afford water oxidation with small overpotential at neutral pH.

In the present communication, we report that the surface modification of a Mn-oxide electrocatalyst with amine-

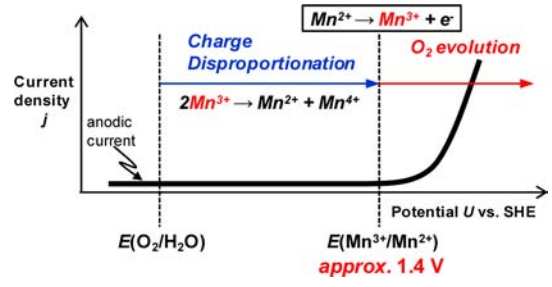

Figure 1. Schematic illustration of a current density (j) vs potential (U) curve for a pristine δ-MnO_2 electrode under neutral pH conditions. The surface-associated intermediate Mn^{3+} species are rapidly consumed by charge disproportionation to form Mn^{2+} and Mn^{4+}, resulting in no net charges passing across the electrode.

Received: July 4, 2012
Published: October 22, 2012

dx.doi.org/10.1021/ja306499n | J. Am. Chem. Soc. 2012, 134, 18153−18156

containing polymers, poly(allylamine hydrochloride) (PAH) is an effective strategy to suppress the CD of Mn^{3+}. Stabilization of Mn^{3+} relative to CD was found to markedly decrease the overpotential for electrochemical water oxidation by MnO_2 at neutral pH, resulting in the initiation of O_2 evolution at a potential near the thermodynamic reversible potential of the four-electron oxidation of H_2O.

A PAH-modified Mn-oxide (PAH-MnO_2) electrode was prepared using a spray deposition method.[25] Briefly, a 0.5 mM colloidal solution of MnO_2 was first obtained by the reduction of $KMnO_4$ with a stoichiometric amount of $Na_2S_2O_3$ at room temperature. An aqueous PAH solution was added under stirring to the colloidal solution (the molar ratio of Mn to the PAH amine group was 5:1), which was then repeatedly sprayed onto a clean conducting glass substrate (FTO-coated glass, resistance: 20 Ω/sq) held on a 200 °C hotplate. The transparent brown film that formed on the electrode was thoroughly rinsed with pure water and then dried at room temperature. The synthesized PAH-MnO_2 electrode exhibited an XRD pattern characteristic of δ-MnO_2 (Figure S1). SEM inspection of the electrode showed that the FTO substrate was uniformly covered with nanoparticles ranging from 20 to 50 nm in diameter (Figure 2A). The uniform distribution of amine

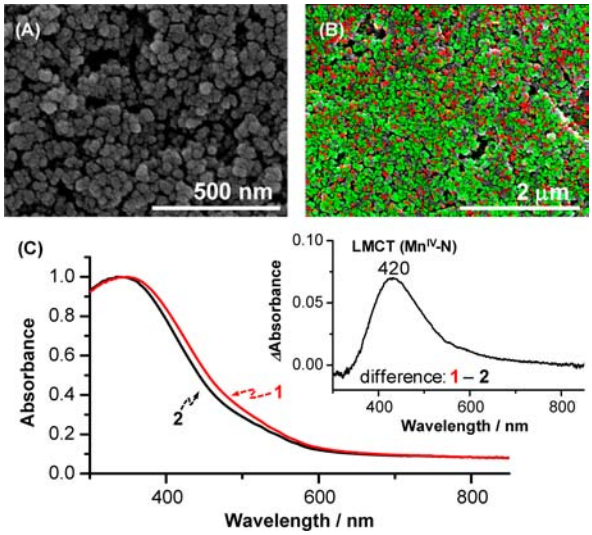

Figure 2. (A) SEM and (B) EDX images of a PAH-MnO_2 film (green, manganese; red, nitrogen). (C) UV−vis absorption spectra of colloidal solutions of (1) PAH-MnO_2 and (2) δ-MnO_2. Inset shows the difference spectrum between (1) and (2).

groups on the electrode surface was evidenced by elemental mapping using energy-dispersive X-ray spectroscopy (Figure 2B).[28] In addition, the formation of N−Mn bonds via the coordination of amine groups to surface Mn sites was revealed by the appearance of a $N^{3-} \rightarrow Mn^{4+}$ LMCT absorption band peak at 420 nm in the optical absorption spectrum of the PAH-MnO_2 electrode (Figure 2C).

Figure 3A shows changes in the diffuse transmission UV−vis absorption spectra of a PAH-MnO_2 electrode at pH 8 (0.5 M Na_2SO_4)[29] over an increasing range of potentials, using spectral data obtained at 0.6 V as a reference. Upon stepping the potential from 0.7 to 1.4 V in 0.1-V increments, a new absorption peak at 470 nm and bleaching of the absorption in the longer-wavelength region of the band-gap transition of MnO_2 were observed. In a previous work, we found that a

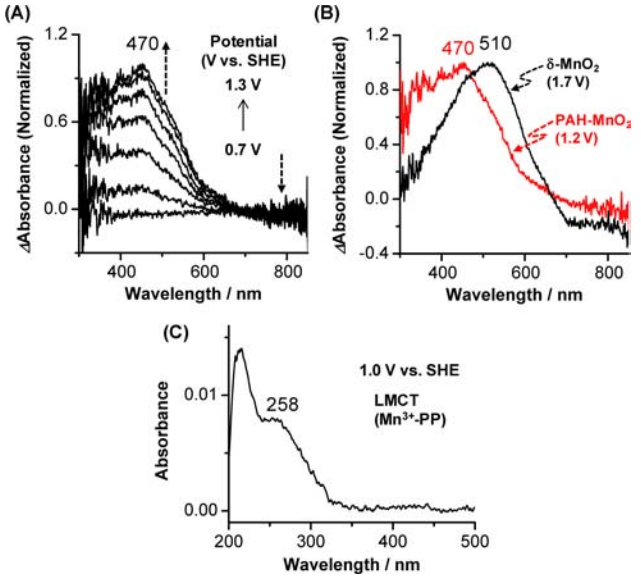

Figure 3. (A) Changes in the diffuse transmission UV−vis spectra of a PAH-MnO_2 film electrode measured at increasing potential (0.7, 0.8, 0.9, 1.0, 1.1, 1.2, and 1.3 V) and pH 8. The spectrum measured at 0.6 V was used as a reference. Dotted arrows indicate the direction of the spectral change with a potential shift from 0.7 to 1.3 V. (B) Comparison of Mn^{3+} d−d transition spectra between PAH-MnO_2 (1.2 V) and pristine δ-MnO_2 (1.7 V) electrodes. The spectra measured at 0.6 and 1.1 V were used as reference spectra for the PAH-MnO_2 and δ-MnO_2 electrode, respectively. (C) UV−vis absorption spectrum of a 20 mM pyrophosphate solution exposed to a PAH-MnO_2 electrode after electrolysis in a 0.5 M Na_2SO_4 solution (pH 8). A 20 mM pyrophosphate solution alone was used as a spectral reference. Electrolysis was conducted for 1 min at an electrode potential of 1.0 V.

pristine δ-MnO_2 electrode exhibited the nearly identical spectral change as a function of potential during the catalytic cycle of water oxidation,[25] except that the absorption band peak formed at 510 nm (Figure 3B, solid black line). The observed shift of the Mn^{3+} d−d transition band from 510 to 470 nm by amine coordination is attributable to the stronger ligand field of PAH amine groups than those of oxide anions. It is noteworthy that a blue shift from 510 to 470 nm was reproduced by treating the surface of pristine δ-MnO_2 with ammonia or imidazole (Figure S2). Thus, the shift in the absorption band is a consequence of N−Mn bond formation.

In Figure 4A, we compared the potential dependence of the 470 and 510 nm absorbance peaks for the PAH-MnO_2 electrode and pristine δ-MnO_2, respectively, from the UV−vis spectroscopy results (Figure 3A). For pristine δ-MnO_2 (black triangles), absorbance at 510 nm was negligible in the potential range of 1.1−1.3 V, but increased at potentials more positive than ∼1.4 V, where Mn^{3+} is forcibly generated by the electrochemical oxidation of Mn^{2+} (see Figure 1). As can be seen from the difference spectrum (Figure 4A, red triangles), the onset potential for Mn^{3+} formation for the PAH-MnO_2 electrode markedly shifted by ∼500 mV in the negative direction relative to that of pristine δ-MnO_2. Notably, the formation of Mn^{3+} for PAH-MnO_2 at more negative potential regions was also demonstrated by probe experiments using PP, a redox-inert molecule that has the ability to uptake Mn^{3+} from the surface of solid-phase Mn oxides via a specific chelating reaction.[30] When the PAH-MnO_2 electrode was immersed into a 20 mM PP solution after electrolysis at 1.0 V for 1 min, Mn^{3+}-PP complexes were detected by optical absorption measure-

dx.doi.org/10.1021/ja306499n | J. Am. Chem. Soc. 2012, 134, 18153−18156

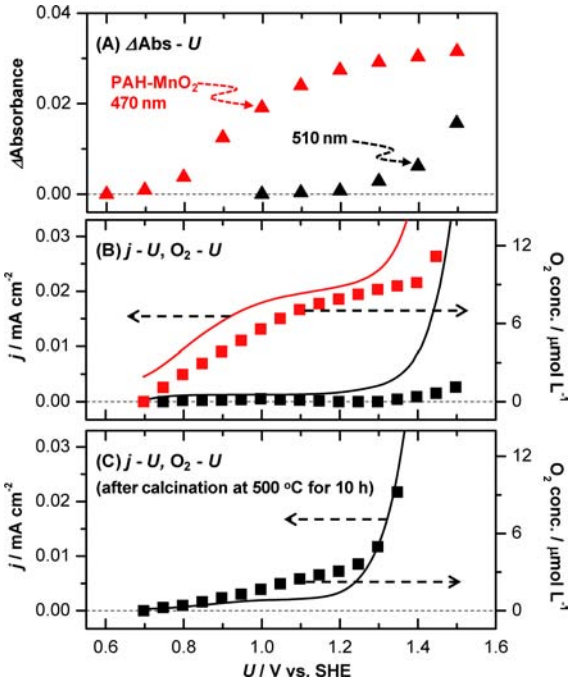

Figure 4. (A) Potential dependences of the difference absorbance for PAH-MnO_2 (470 nm) and pristine δ-MnO_2 (510 nm) electrodes, respectively, measured at pH 8. (B) Current density (solid line) and dissolved O_2 concentration (filled squares) for PAH-MnO_2 and pristine δ-MnO_2 electrodes at pH 8. Solid red line and squares: PAH-MnO_2; solid black line and squares: pristine δ-MnO_2. (C) Potential dependences of current density (solid line) and dissolved O_2 concentration (filled squares) for a PAH-MnO_2 electrode after calcination at 500 °C for 10 h.

ments[30,31] (Figure 3C). Therefore, we can conclude that Mn^{3+} species are effectively stabilized by the formation of N−Mn bonds via the coordination of PAH amine groups with the surface Mn sites of MnO_2 electrodes.

To confirm the effects of stabilization of Mn^{3+} ions against CD on O_2 evolution activity, a PAH-MnO_2 electrode was subjected to electrochemical water oxidation at pH 8[29] (Figure 4B). The amount of dissolved oxygen was monitored simultaneously with current density (j) versus potential (U) measurements using a needle-type oxygen microsensor. Interestingly, upon sweeping the electrode potential, an increase in both anodic current (solid red line) and O_2 production (red squares) was observed at an onset potential of close to 0.8 V. This potential is ∼500 mV more negative than the corresponding values for a pristine δ-MnO_2 electrode (solid black line and black squares, respectively) and is nearly identical with the onset potential of Mn^{3+} production for a PAH-MnO_2 electrode (Figure 4A, red triangles). It should be noted that when PAH coated on the MnO_2 electrode surface was decomposed by calcination of the electrode at 500 °C,[32] both the anodic current and O_2 production were largely suppressed in the potential range of 0.8−1.3 V (Figure 4C). Calcination of the PAH-MnO_2 electrode at 500 °C also suppressed the production of Mn^{3+} in this potential range (see Figure S6). A strong correlation was detected between the onset potentials of O_2 evolution and Mn^{3+} production, both before (Figure 4A,B) and after (Figures 4C and S6) the thermal decomposition of PAH. Therefore, the UV−vis spectroscopy results and observed onsets potentials provide strong support for the hypothesis that the stabilization of Mn^{3+} effectively lowers the overpotential required for electrochemical water oxidation by MnO_2.

The current efficiency (CE) for water oxidation by a PAH-MnO_2 electrode was estimated using quadrupole mass spectroscopy. The electrolysis at 1.0 V for 1 h showed an increase in mass peaks assigned to N_2 and O_2. The CE for O_2 evolution was estimated to 20%. Production of N_2 indicates that the oxidation of amine groups of PAH polymer proceeds simultaneously with water oxidation.[33]

Concerning the mechanisms of Mn^{3+} stabilization, it is worth noting that CD is a competing process to Jahn−Teller (JT) distortion for eliminating orbital degeneracy.[34−38] As the trivalent state of Mn in δ-MnO_2 adopts a high-spin d^4 configuration ($t_{2g}^3e_g^1$),[39] $Mn^{3+}O_6$ octahedra are typically subjected to JT distortion. On one hand, the Mn^{2+} and Mn^{4+} produced by the CD of Mn^{3+} adopt nondegenerate $t_{2g}^3e_g^2$ and $t_{2g}^3e_g^0$ configurations, respectively. Therefore, the Mn^{3+} in δ-MnO_2 is able to eliminate orbital degeneracy by CD. As demonstrated in the difference spectra (Figure 4A), the formation of N−Mn bonds on the MnO_2 electrode surface effectively suppresses the CD of Mn^{3+}, resulting in the accumulation of Mn^{3+} on the electrode surface even at potentials more negative than 1.4 V. Therefore, we consider that asymmetrization of the Mn-centered crystal field via N−Mn bond formation, which was evidenced by the blue shift of the d−d transition band of Mn^{3+} through amine coordination (Figure 3B), favors JT distortion over CD as the mechanism to eliminate the orbital degeneracy of Mn^{3+}.

In summary, the present *in situ* spectroelectrochemical detection of surface intermediates formed during the water oxidation reaction by a MnO_2 electrocatalyst has demonstrated for the first time that a strong correlation exists between the onset potentials of O_2 evolution and Mn^{3+} production. The formation of N−Mn bonds via the coordination of amine groups to the surface Mn sites of MnO_2 electrodes was found to stabilize the Mn^{3+} species, resulting in O_2 production at an onset potential close to the thermodynamic reversible potential of the four-electron oxidation of H_2O, $E(O_2/H_2O)$ = 0.76 V, at pH 8. This finding supports our hypothesis that suppression of the CD of Mn^{3+} is essential to lower the overpotential for electrochemical water oxidation by MnO_2 at neutral pH.[25] To eliminate the orbital degeneracy of Mn^{3+} ($t_{2g}^3e_g^1$), CD is an alternative to JT distortion.[34−38] Thus, the introduction of asymmetry into the Mn-centered crystal field demonstrated in this work represents a new design principle for efficient multielectron water oxidation catalysts composed of inexpensive and abundant MnO_2 for artificial photosynthesis.

■ ASSOCIATED CONTENT

Supporting Information

Experimental details, XRD pattern of PAH-MnO_2, *in situ* UV−vis absorption spectra of MnO_2 coordinated with imidazole or ammonia, TGA profile of PAH, and additional plots of difference absorbance as a function of electrode potential using a PAH-MnO_2 electrode after calcination. This material is available free of charge via the Internet at http://pubs.acs.org.

■ AUTHOR INFORMATION

Corresponding Author

hashimoto@light.t.u-tokyo.ac.jp; nakamura@light.t.u-tokyo.ac.jp

Present Address
[§]National Institute for Materials Science (NIMS), 1-1 Namiki, Ibaraki, 305-0044, Japan

Notes
The authors declare no competing financial interest.

■ ACKNOWLEDGMENTS

This work was financially supported by the Exploratory Research for Advanced Technology (ERATO) program of the Japan Science and Technology Agency (JST), and partially by a Grant-in-Aid for Scientific Research on Priority Areas from the Ministry of Education, Culture, Sports, Science, Technology (MEXT) of the Japanese Government (21750186), The Canon Foundation, and Research Fellowships of the Japan Society for Promotion of Science (JSPS) for Young Scientists (21•9161).

■ REFERENCES

(1) Alstrum-Acevedo, J. H.; Brennaman, M. K.; Meyer, T. J. *Inorg. Chem.* **2005**, *44*, 6802.
(2) Jiao, F.; Frei, H. *Energy Environ. Sci.* **2010**, *3*, 1018.
(3) Dismukes, G. C.; Brimblecombe, R.; Felton, G. A. N.; Pryadun, R. S.; Sheats, J. E.; Spiccia, L.; Swiegers, G. F. *Acc. Chem. Res.* **2009**, *42*, 1935.
(4) Zhao, Y.; Hernandez-Pagan, A. E.; Vargas-Barbosa, M. N.; Dysart, L. J.; Mallouk, E. T. *J. Phys. Chem. Lett.* **2011**, *2*, 402.
(5) Zhang, F.; Yamakata, A.; Maeda, K.; Moriya, Y.; Takata, T.; Kubota, J.; Teshima, K.; Oishi, S.; Domen, K. *J. Am. Chem. Soc.* **2012**, *134*, 8348.
(6) Abe, R.; Higashi, M.; Domen, K. *J. Am. Chem. Soc.* **2010**, *132*, 11828.
(7) Duan, L.; Bozoglian, F.; Mandal, S.; Stewart, B.; Privalov, T.; Llobet, A.; Sun, L. *Nat. Chem.* **2012**, *4*, 418.
(8) Yin, Q.; Tan, M. J.; Besson, C.; Geletii, V. Y.; Musaev, G. D.; Kuznetsov, E. A.; Luo, Z.; Hardcastle, I. K.; Hill, L. C. *Science* **2010**, *328*, 342.
(9) Fillol, L. J.; Codolà, Z.; Garcia-Bosch, I.; Pla, J. J.; Costas, M. *Nat. Chem.* **2011**, *3*, 807.
(10) Umena, Y.; Kawakami, K.; Shen, J. R.; Kamiya, N. *Nature* **2011**, *473*, 55.
(11) Yano, J.; Kern, J.; Sauer, K.; Latimer, J. M.; Pushkar, Y.; Biesiadka, J.; Loll, B.; Saenger, W.; Messinger, J.; Zouni, A.; Yachandra, K. V. *Science* **2006**, *314*, 821.
(12) Siegbahn, E. M. P. *Acc. Chem. Res.* **2009**, *42*, 1871.
(13) Armstrong, A. F. *Philos. Trans. R. Soc., B* **2008**, *363*, 1263.
(14) Wiechen, M.; Berends, H.; Kurz, P. *Dalton Trans.* **2012**, *41*, 21.
(15) Robinson, D. M.; Go, Y. B.; Greenblatt, M.; Dismukes, G. C. *J. Am. Chem. Soc.* **2010**, *132*, 11467.
(16) Yagi, M.; Toda, M.; Yamada, S.; Yamazaki, H. *Chem. Commun.* **2010**, *46*, 8594.
(17) Shimazaki, Y.; Nagano, T.; Takesue, H.; Ye, B. H.; Tani, F.; Naruta, Y. *Angew. Chem., Int. Ed.* **2004**, *43*, 98.
(18) Suntivich, J.; May, J. K.; Gasteiger, A. H.; Goodenough, B. J; Shao-Horn, Y. *Science* **2011**, *334*, 1383.
(19) Najafpour, M. M.; Ehrenberg, T.; Wiechen, M.; Kurz, P. *Angew. Chem., Int. Ed.* **2010**, *49*, 2233.
(20) Jiao, F.; Frei, H. *Chem. Commun.* **2010**, *46*, 2920.
(21) Iyer, A.; Del-Pilar, J.; King'ondu, K. C.; Kissel, E.; Garces, F. H.; Huang, H.; El-Sawy, M. A.; Dutta, K. P.; Suib, L. S. *J. Phys. Chem. C* **2012**, *116*, 6474.
(22) Gorlin, Y.; Jaramillo, T. F. *J. Am. Chem. Soc.* **2010**, *132*, 13612.
(23) Cheng, F.; Shen, J.; Peng, B.; Pan, Y.; Tao, Z.; Chen, J. *Nat. Chem.* **2011**, *3*, 79.
(24) Ramírez, A.; Bogdanoff, P.; Friedrich, D.; Fiechter, S. *Nano Energy* **2012**, *1*, 282.
(25) Takashima, T.; Hashimoto, K.; Nakamura, R. *J. Am. Chem. Soc.* **2012**, *134*, 1519.
(26) Silvester, E.; Manceau, A.; Drits, V. *Am. Mineral.* **1997**, *82*, 962.
(27) Baral, S.; Lume-Pereira, C.; Janata, E.; Henglein, A. *J. Phys. Chem.* **1985**, *89*, 5779.
(28) From the EDX analysis shown in Figure 2B, the surface coverage of amine groups of PAH was estimated to approximately 30%.
(29) The pH of the electrolyte was adjusted using 0.1 M H_2SO_4 and 1.0 M NaOH, and their mixture. No agent for pH buffering was added to avoid influences from the specific adsorption of multivalent anions.
(30) Webb, M. S.; Dick, J. G.; Bargar, R. J.; Tebo, M. B. *Proc. Natl. Acad. Sci. U.S.A.* **2005**, *102*, 5558.
(31) We employed the 258-nm absorption peak as a spectroscopic signature for Mn^{3+}-PP formation. The 258-nm absorption is assigned to LMCT for the Mn^{3+}-PP complex.
(32) We observed that PAH was completely decomposed at 500 °C using thermogravimetric analysis (TGA; see Figure S5).
(33) The current density of a PAH-MnO_2 electrode decreased gradually with time due to the decomposition of PAH polymer during water oxidation (Figure S8). It was confirmed that a PAH-MnO_2 electrode preserved the effects of N-coordination on current generation for at least 1 h at 1.0 V.
(34) Mazin, I. I.; Lengsdorf, R.; Alonso, J. A.; Marshall, W. G.; Ibbreson, R. M.; Podlesnyak, A.; Martínez-Lope, M. J.; Abd-Elmeguid, M. M. *Phys. Rev. Lett.* **2007**, *98*, 176406.
(35) Whangbo, M. H.; Koo, H. J.; Villesuzanne, A.; Pouchard, M. *Inorg. Chem.* **2002**, *41*, 1920.
(36) Hao, X.; Xu, Y.; Gao, F.; Zhou, D.; Meng, J. *Phys. Rev. B* **2009**, *79*, 113101.
(37) Mizokawa, T.; Khomskii, D. I.; Sawatzky, G. A. *Phys. Rev. B* **2000**, *61*, 11263.
(38) Chen, H.; Freeman, C. L.; Harding, J. H. *Phys. Rev. B* **2011**, *84*, 085108.
(39) Sakai, N.; Ebina, Y.; Takada, K.; Sasaki, T. *J. Phys. Chem. B* **2005**, *109*, 9651.